Обзор ArXiv/astro-ph, 9-13 ноября 2020

От Сильченко О.К.

ArXiv: 2011.05340

Fast rotating and low-turbulence discs at $z \simeq 4.5$: dynamical evidence of their evolution into local early-type galaxies.

F. Fraternali[1], A. Karim[2], B. Magnelli[2], C. Gómez-Guijarro[3], E. F. Jiménez-Andrade[4], and A. C. Posses[5]

[1] Kapteyn Astronomical Institute, University of Groningen, Postbus 800, 9700 AV Groningen, The Netherlands, e-mail: fraternali@astro.rug.nl
[2] Argelander Institut für Astronomie, Universität Bonn, Auf dem Hügel 71, Bonn, D-53121, Germany.
[3] AIM, CEA, CNRS, Université Paris-Saclay, Université Paris Diderot, Sorbonne Paris Cité, F-91191 Gif-sur-Yvette, France.
[4] National Radio Astronomy Observatory, 520 Edgemont Road, Charlottesville, VA 22903, USA.
[5] Núcleo de Astronomía, Facultad de Ingeniería y Ciencias, Universidad Diego Portales, Av. Ejército 441, Santiago, Chile.

Received ; accepted

ABSTRACT

Massive starburst galaxies in the early Universe are estimated to have depletion times of ~ 100 Myr and thus be able to convert their gas very quickly into stars, possibly leading to a rapid quenching of their star formation. For these reasons they are considered progenitors of massive early-type galaxies (ETGs). In this paper, we study two high-z starbursts, AzTEC/C159 ($z \simeq 4.57$) and J1000+0234 ($z \simeq 4.54$), observed with ALMA in the [C II] 158-μm emission line. These observations reveal two massive and regularly rotating gaseous discs. A 3D modelling of these discs returns rotation velocities of about 500 km s^{-1} and gas velocity dispersions as low as ≈ 20 km s^{-1}, at least in AzTEC/C159, leading to very high ratios between regular and random motion ($V/\sigma \gtrsim 20$). The mass decompositions of the rotation curves show that both galaxies are highly baryon-dominated with gas masses of $\approx 10^{11}\ M_{\odot}$, which, for J1000+0234, is significantly higher than previous estimates. We show that these high-z galaxies overlap with $z = 0$ massive ETGs in the ETG-analogue of the Tully-Fisher relation once their gas is converted into stars. This provides a dynamical evidence of the connection between massive high-z starbursts and ETGs, although the transformation mechanism from fast-rotating to nearly pressure-supported systems remains unclear.

Две массивных галактики со звездообразованием (SMG?)

Table 1. Physical properties of AzTEC/C159

Property	Value	Ref
Kinematic centre (R.A.)	$9^h\,59^m\,30.40^s \pm 0.03^s$	1
Kinematic centre (Dec.)	$+1°\,55'\,27.57'' \pm 0.05''$	1
z	4.5668 ± 0.0002	1
Stellar mass ($M_\star$)	$4.5 \pm 0.4 \times 10^{10}\,M_\odot$	2
Star form. rate (SFR)	$740^{+210}_{-170}\,M_\odot\,\mathrm{yr}^{-1}$	3
Mol. gas mass (M_{H_2})	$1.5 \pm 0.3 \times 10^{11}\,M_\odot$	3
Disc inclination (i)	$40 \pm 10°$	1
Disc position angle (PA)	$170 \pm 10°$	1
[C II] 158-μm flux	$4.6\,\mathrm{Jy\,km\,s}^{-1}$	1
Rotation velocity (v_{rot})	$506^{+151}_{-76}\,\mathrm{km\,s}^{-1}$	1
Velocity dispersion (σ_{gas})	$16 \pm 13\,\mathrm{km\,s}^{-1}$	1
Conversion $''$/ kpc	6.70	

References. (1) This work; (2) Gómez-Guijarro et al. (2018); (3) Jiménez-Andrade et al. (2018).

Table 2. Physical properties of J1000+0234

Property	Value	Ref
Kinematic centre (R.A.)	$10^h\,0^m\,54.48^s \pm 0.03^s$	1
kinematic centre (Dec.)	$+2°\,34'\,36.12'' \pm 0.05''$	1
z	4.5391 ± 0.0004	1
Stellar mass ($M_\star$)	$(1.4 - 8.6) \times 10^{10}\,M_\odot$	2, 3
Star form. rate (SFR)	$440^{+1200}_{-320}\,M_\odot\,\mathrm{yr}^{-1}$	2
Mol. gas mass (M_{H_2})	$(2.6 - 10) \times 10^{10}\,M_\odot$	4,1
Disc inclination (i)	$75 \pm 10°$	1
Disc position angle (PA)	$145 \pm 5°$	1
[C II] 158-μm flux	$5.9\,\mathrm{Jy\,km\,s}^{-1}$	1
Rotation velocity (v_{rot})	$538 \pm 40\,\mathrm{km\,s}^{-1}$	1
Velocity dispersion (σ_{gas})	$\lesssim 60\,\mathrm{km\,s}^{-1}$	1
Conversion $''$/kpc	6.72	

References. (1) This work; (2) Gómez-Guijarro et al. (2018); (3) Smolčić et al. (2015); (4) Schinnerer et al. (2008).

Поле скоростей в [CII] для AzTEC/C159

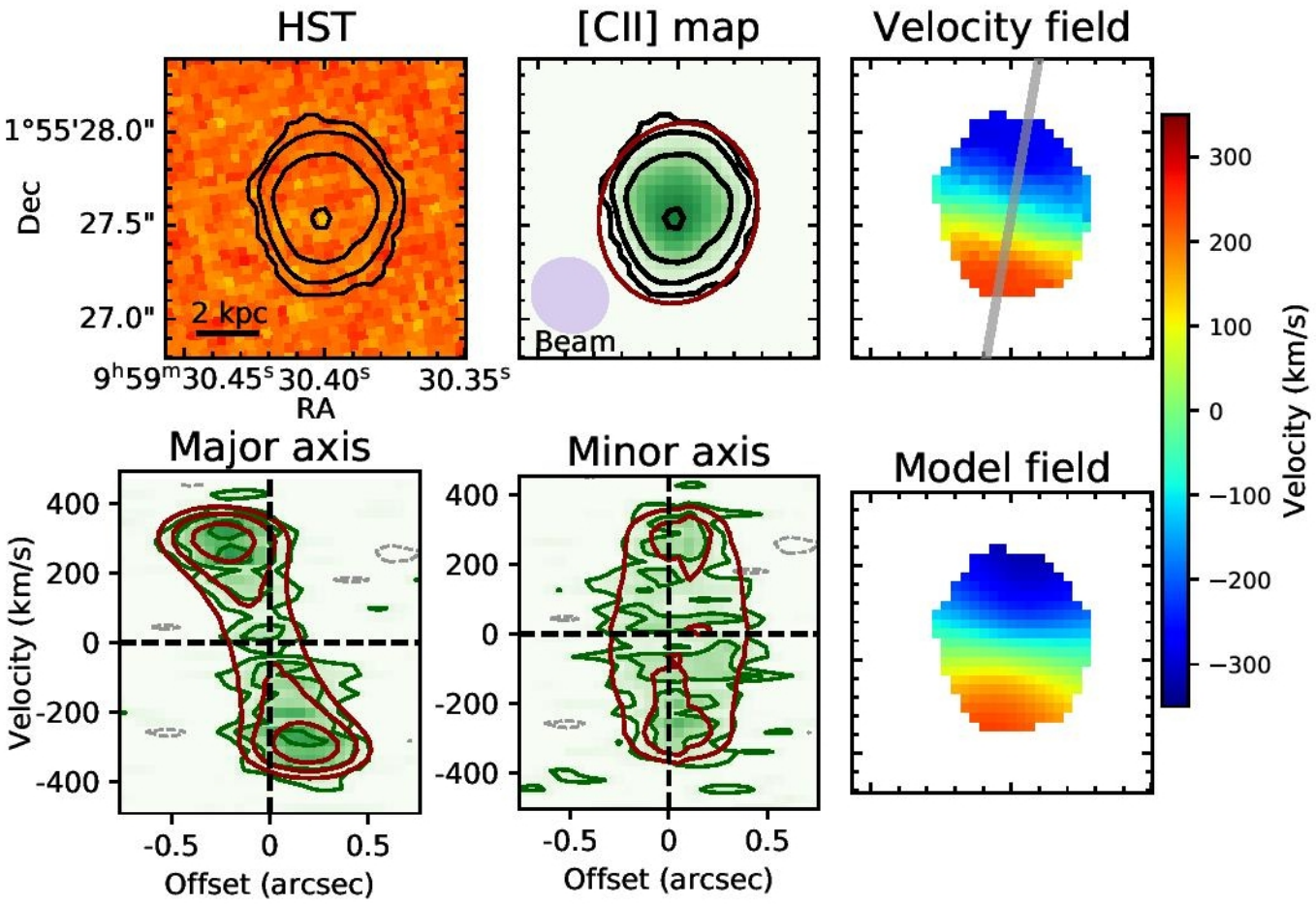

Ее кривая вращения и дисперсия скоростей газа

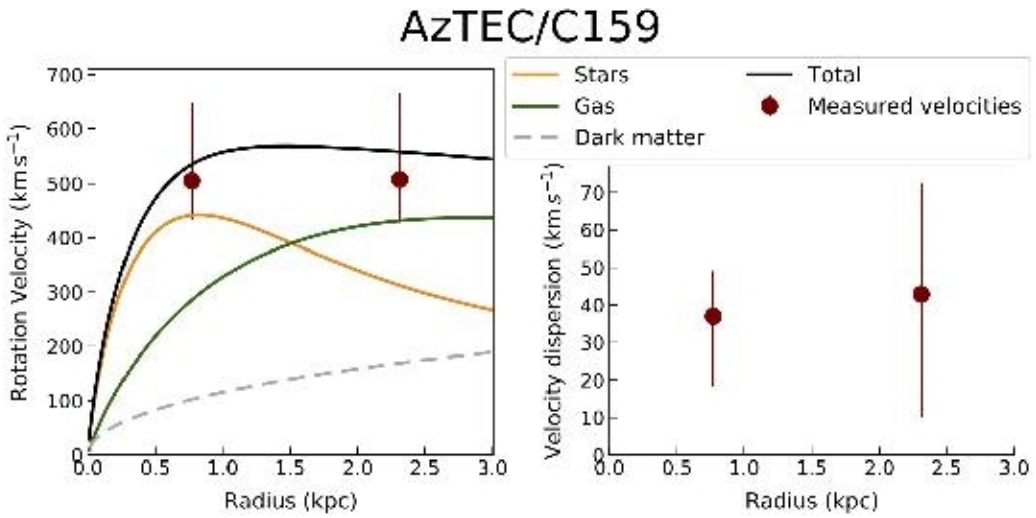

Fig. 3. *Left panel*: Rotation velocity of the two rings/annuli in which we decomposed the disc of AzTEC/C159. The orange and green curves show the contribution of, respectively, stars and gas modelled as exponential discs, the grey dashed curve shows that of a dark matter halo modelled as a NFW profile and the black curve is the sum of all components. *Right panel*: Gas velocity dispersion in the two annuli obtained using the low spectral resolution datacube (see Section 3.5 for the high resolution values).

Поле скоростей в [CII] для J1000+0234

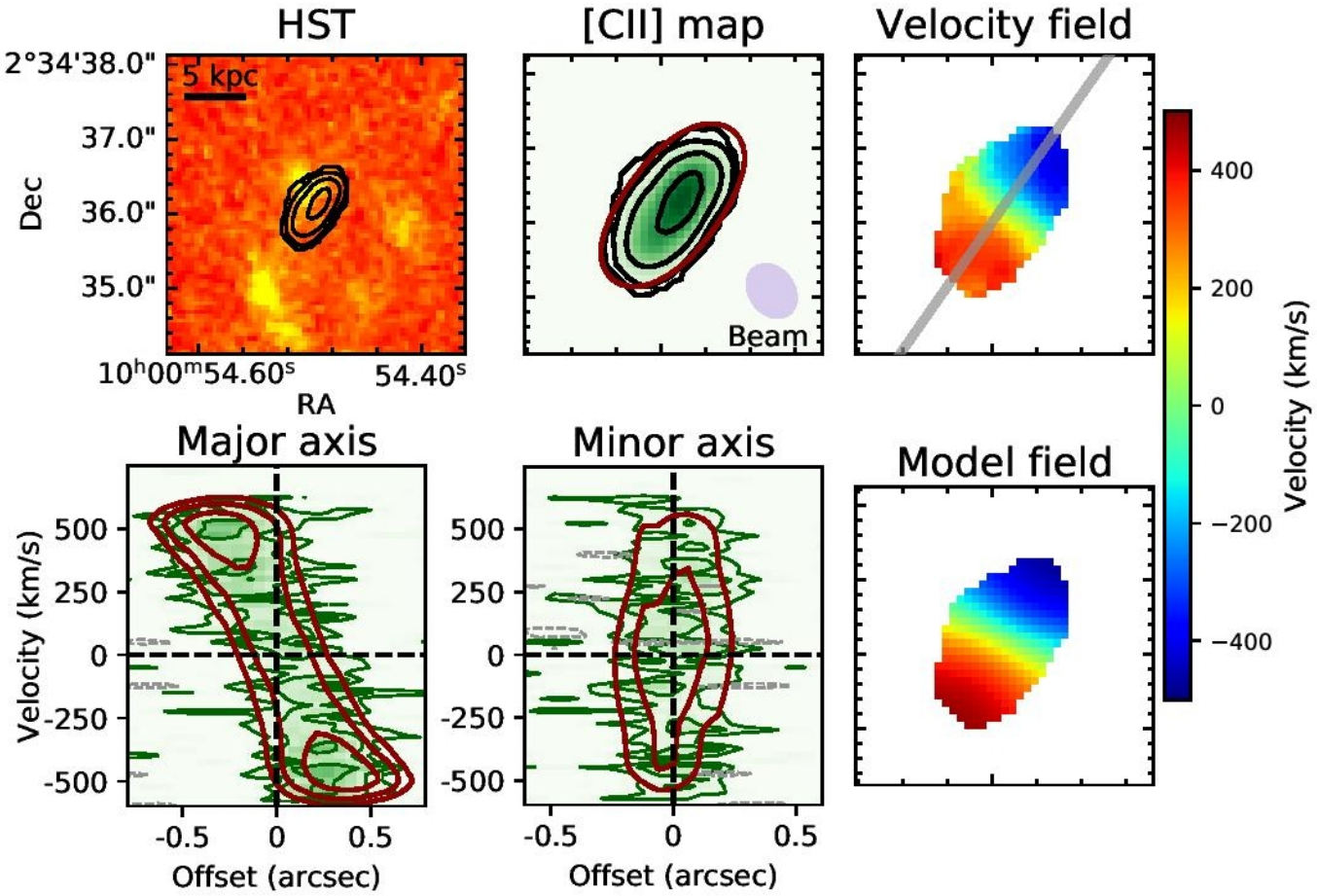

Ее кривая вращения и дисперсия скоростей газа

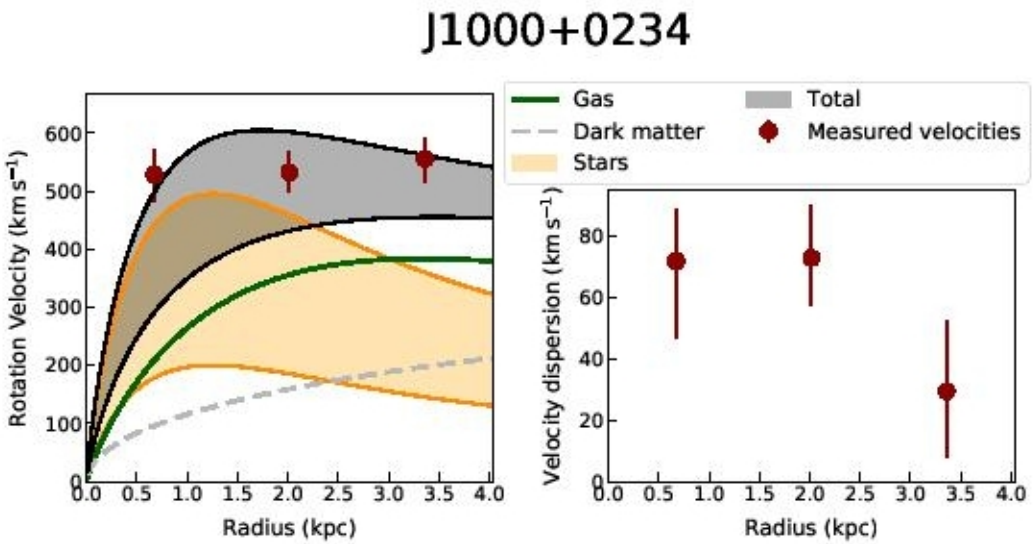

Fig. 6. *Left panel*: Rotation velocities measured in J1000+0234 (red points) compared to the contributions of different matter components. This comparison is illustrative and not fitted to the data points. Orange lines and shade: contribution of the stellar component given the two estimates of stellar mass present in the literature. Green solid curve: contribution of the gas disc, assumed exponential and derived from the [C II] 158-μm distribution. Grey dashed curve: contribution of a dark matter halo given by an NFW profile with a mass of $M_{200} = 2\times10^{12}\,M_{\odot}$. Black lines and shade: total contribution of all components. *Right panel*: [C II] velocity dispersion in J1000+0234.

Для оценки дисперсии скоростей надо бы разрешение лучше:27→10km/s

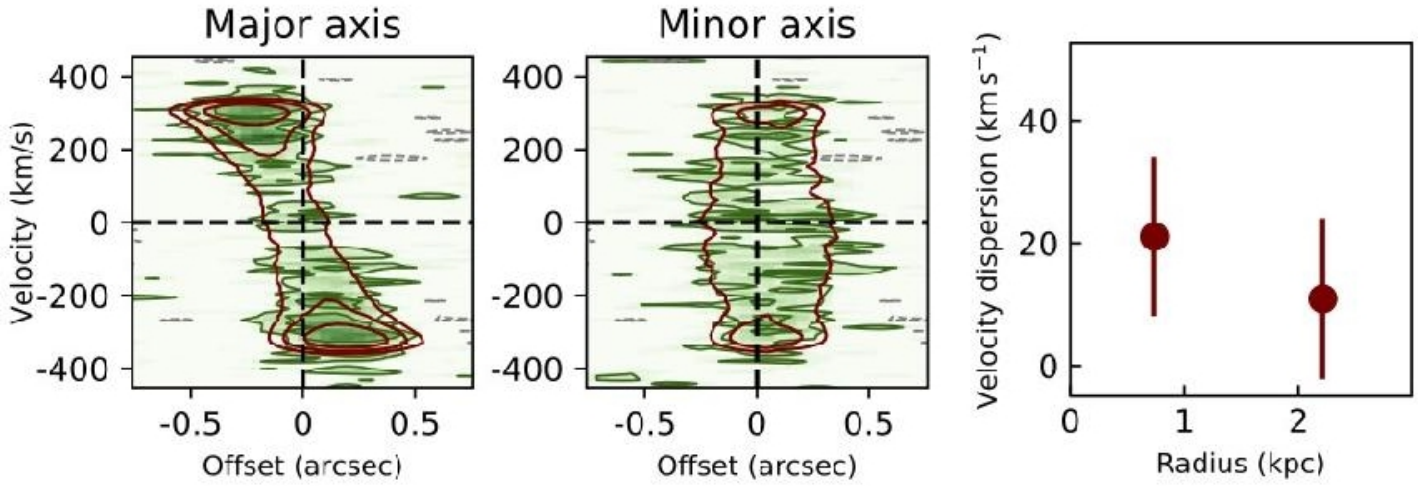

Fig. 7. *Left panel*: Position-velocity diagram along the kinematic major axis of AzTEC/C159 (see Fig. 1) obtained using the high spectral resolution datacube (Table 3). The [C II] 158-μm emission in the data is in green shade and contours, while the ^{3D}BAROLO model is in red contours. Contour levels are at −2, 2, 4 and 8 times the r.m.s. noise per channel. *Centre panel*: Position-velocity diagram along the kinematic minor axis displayed analogously to the major-axis plot. *Right panel*: [C II] velocity dispersion obtained from the high spectral resolution datacube.

Спекуляция: что будет дальше

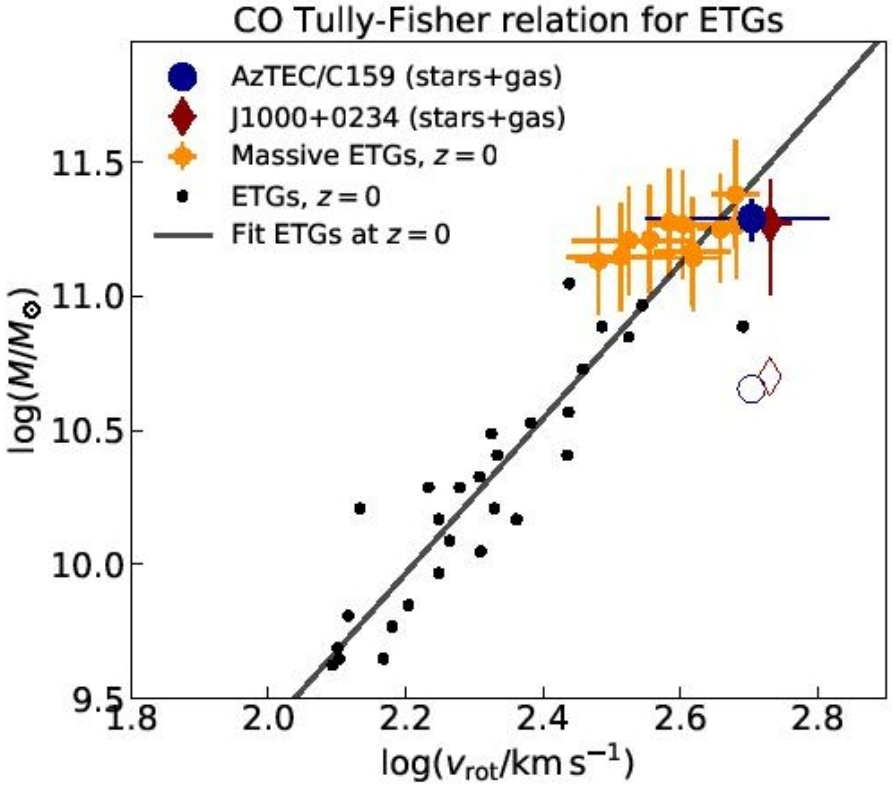

Fig. 9. Tully-Fisher (analogue) relation for ETGs at $z = 0$ from Davis et al. (2016) compared with the positions of our starburst galaxies at $z \approx 4.5$. In the local ETGs the rotational speed is derived from the inner CO discs, while in our galaxies is obtained from the [C II] line. The empty symbols show the positions of our galaxies based on the observed stellar mass, while the filled symbols shows their positions assuming that all the observed gas mass is converted into stars.

ArXiv: 2011.03736

THE SAMI GALAXY SURVEY: STELLAR POPULATIONS OF PASSIVE SPIRAL GALAXIES IN DIFFERENT ENVIRONMENTS

Mina Pak[1,2], Sree Oh[3,4], Joon Hyeop Lee[1,2], Nicholas Scott[4,5], Rory Smith[1], Jesse van de Sande[4,5], Scott M. Croom[4,5], Francesco D'Eugenio[6], Kenji Bekki[7], Sarah Brough[4,8], Caroline Foster[4,5], Tania M. Barone[3,4,5], Katarina Kraljic[9], Hyunjin Jeong[1], Joss Bland-Hawthorn[5], Julia J. Bryant[4,5,10], Michael Goodwin[4,5,11], Jon Lawrence[12], Matt S. Owers[13,14], Samuel N. Richards[15]

[1]Korea Astronomy and Space Science Institute (KASI), 776 Daedukdae-ro, Yuseong-gu, Daejeon 34055, Republic of Korea
[2]University of Science and Technology, Korea (UST), 217 Gajeong-ro Yuseong-gu, Daejeon 34113, Republic of Korea
[3]Research School of Astronomy and Astrophysics, Australian National University, Canberra, ACT 2611, Australia
[4]ARC Centre of Excellence for All Sky Astrophysics in 3 Dimensions (ASTRO 3D), Australia
[5]Sydney Institute for Astronomy (SIfA), School of Physics, University of Sydney, NSW 2006, Australia
[6]Sterrenkundig Observatorium, Universiteit Gent, Krijgslaan 281 S9, B-9000 Gent, Belgium
[7]ICRAR M468, The University of Western Australia, 35 Stirling Hwy, Crawley, Western Australia 6009, Australia
[8]School of Physics, University of New South Wales, NSW 2052, Australia
[9]Institute for Astronomy, Royal Observatory, Edinburgh EH9 3HJ, UK
[10]Australian Astronomical Optics, AAO-USydney, School of Physics, University of Sydney, NSW 2006, Australia
[11]Australian Astronomical Optics – Macquarie, 105 Delhi Rd, North Ryde, NSW 2113, Australia
[12]Australian Astronomical Optics - Macquarie, Macquarie University, NSW 2109, Australia
[13]Department of Physics and Astronomy, Macquarie University, NSW 2109, Australia
[14]Astronomy, Astrophysics and Astrophotonics Research Centre, Macquarie University, Sydney, NSW 2109, Australia and
[15]SOFIA Science Center, USRA, NASA Ames Research Center, Building N232, M/S 232-12, P.O. Box 1, Moffett Field, CA 94035-0001, USA

Draft version November 10, 2020

ABSTRACT

We investigate the stellar populations of passive spiral galaxies as a function of mass and environment, using integral field spectroscopy data from the Sydney-AAO Multi-object Integral field spectrograph Galaxy Survey. Our sample consists of 52 cluster passive spirals and 18 group/field passive spirals, as well as a set of S0s used as a control sample. The age and [Z/H] estimated by measuring

Обзор галактик SAMI с IFU

SAMI was mounted on the 3.9m Anglo-Australian Telescope (Croom et al. 2012). The instrument is characterized by 13 fused optical fibre bundles (hexabundles), each one containing 61 fibres of 1.6″ diameter resulting in each Integral Field Unit (IFU) having a 15″ diameter (Bland-Hawthorn et al. 2011; Bryant et al. 2014). The SAMI fibres are fed into the two arms of the AAOmega spectrograph (Sharp et al. 2006). The SAMI Galaxy Survey uses the 580V grating in the blue arm resulting in a resolution R=1812 and wavelength coverage of 3700-5700 Å, and the 1000R grating in the red arm resulting in the higher resolution R=4263 over the range 6300-7400 Å. The median full-width-at-half-maximum values for each arm are FWHM_{blue}=2.65 Å and FWHM_{red}=1.61 Å (van de Sande et al. 2017a).

The SAMI Galaxy Survey is a spatially-resolved spectroscopic survey of more than 3000 galaxies collected during 2013-2018, with stellar mass range $\log(M_*/M_\odot) = 8 - 12$ and redshift range $0.004 < z \leq 0.115$ (Bryant et al. 2015). The data are reduced using the SAMI PYTHON package (Allen et al. 2014) which includes the 2dFDR package (AAO Software Team 2015).

Пассивные спирали (?)

FIG. 1.— The DECam Legacy Survey (DECaLS) images of the passive spiral galaxies in the SAMI-cluster (top row) and the SAMI-GAMA samples (bottom row). The image size is $100'' \times 100''$. The ID of the SAMI galaxies is shown in the top corner of each galaxy.

52 в скоплениях, 18 в поле

Характеристики (вместе с S0)

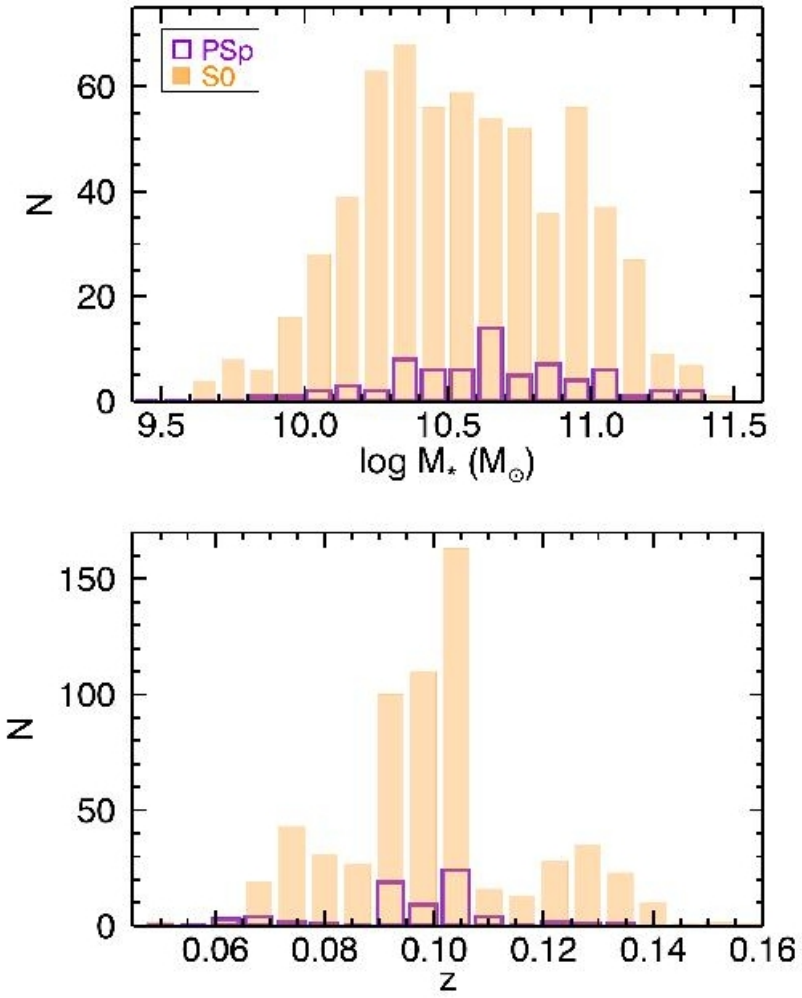

FIG. 3.— The distributions of the stellar mass and redshift for

Таки да, звездообразования нет ни в тех, ни в других

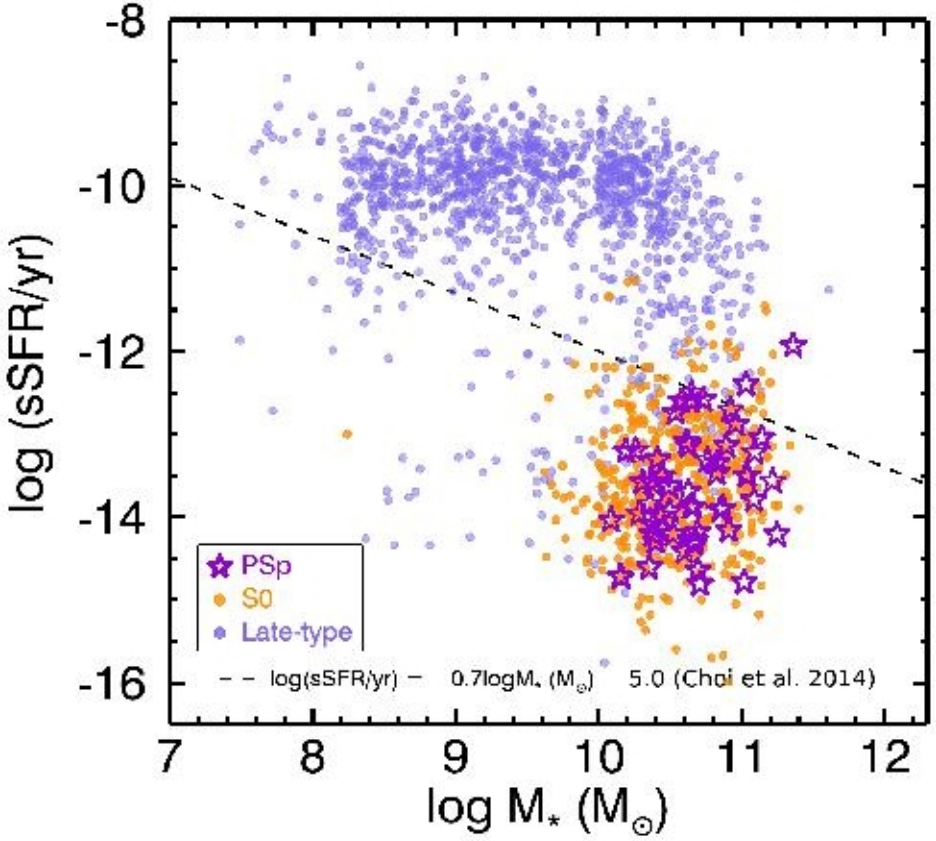

Ликские индексы: результат для галактик в скоплениях

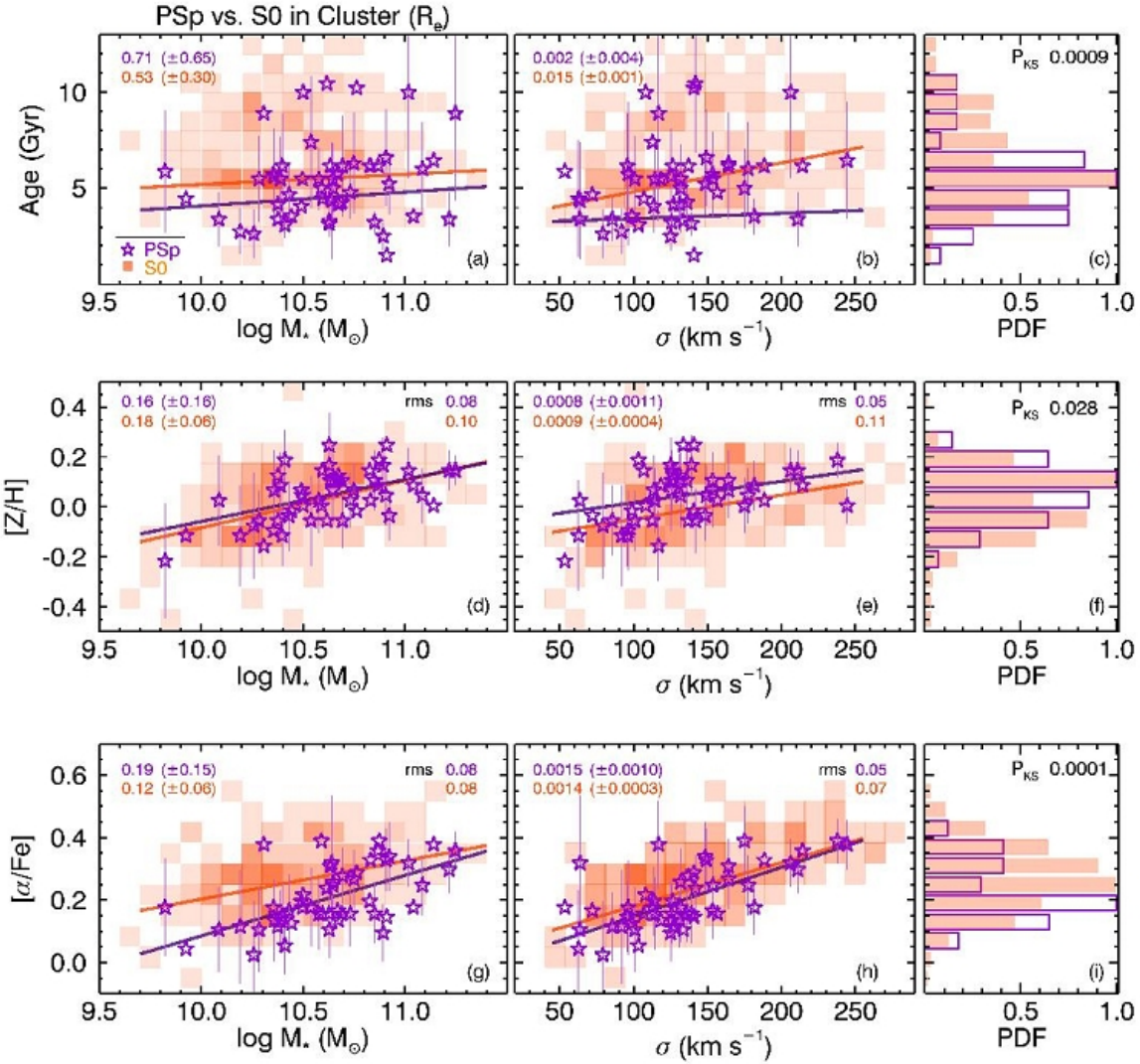

FIG. 6.— Age (top), [Z/H] (middle), and [α/Fe] (bottom) as a function of stellar mass and $\sigma_\star$ within R_e for the cluster sample, compared between the cluster passive spirals (stars) and the S0s (colorscale). Solid lines are linear-fits by weighted errors using the MPFIT function (Markwardt 2009) in IDL library. The slope of the fit is presented in the top left corner of the panels. For passive spirals and S0s more

Ликские индексы: результат для галактик в поле

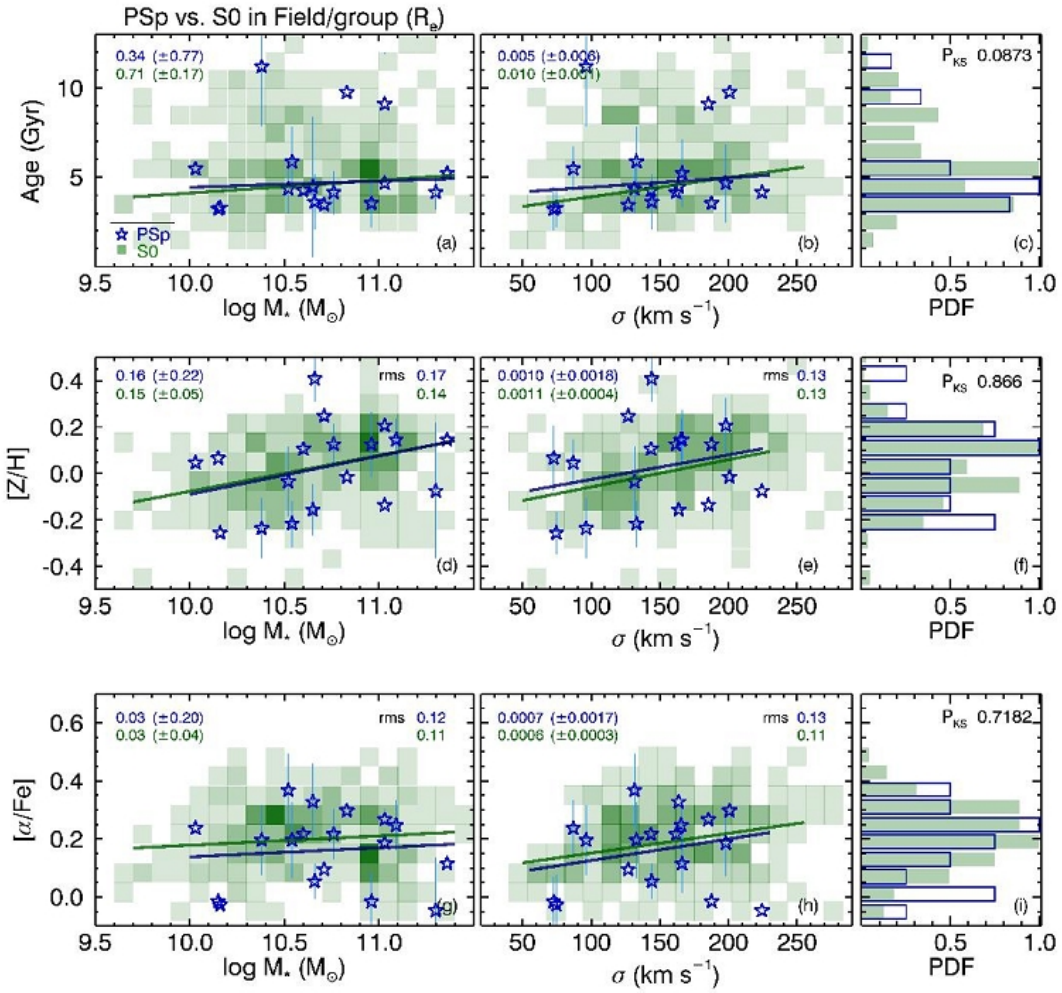

FIG. 7.— The same as Figure 6 but for the field/group passive spirals and S0s. In histogram, the blue and green bins show passive spirals and S0s, respectively.

А сравнить?

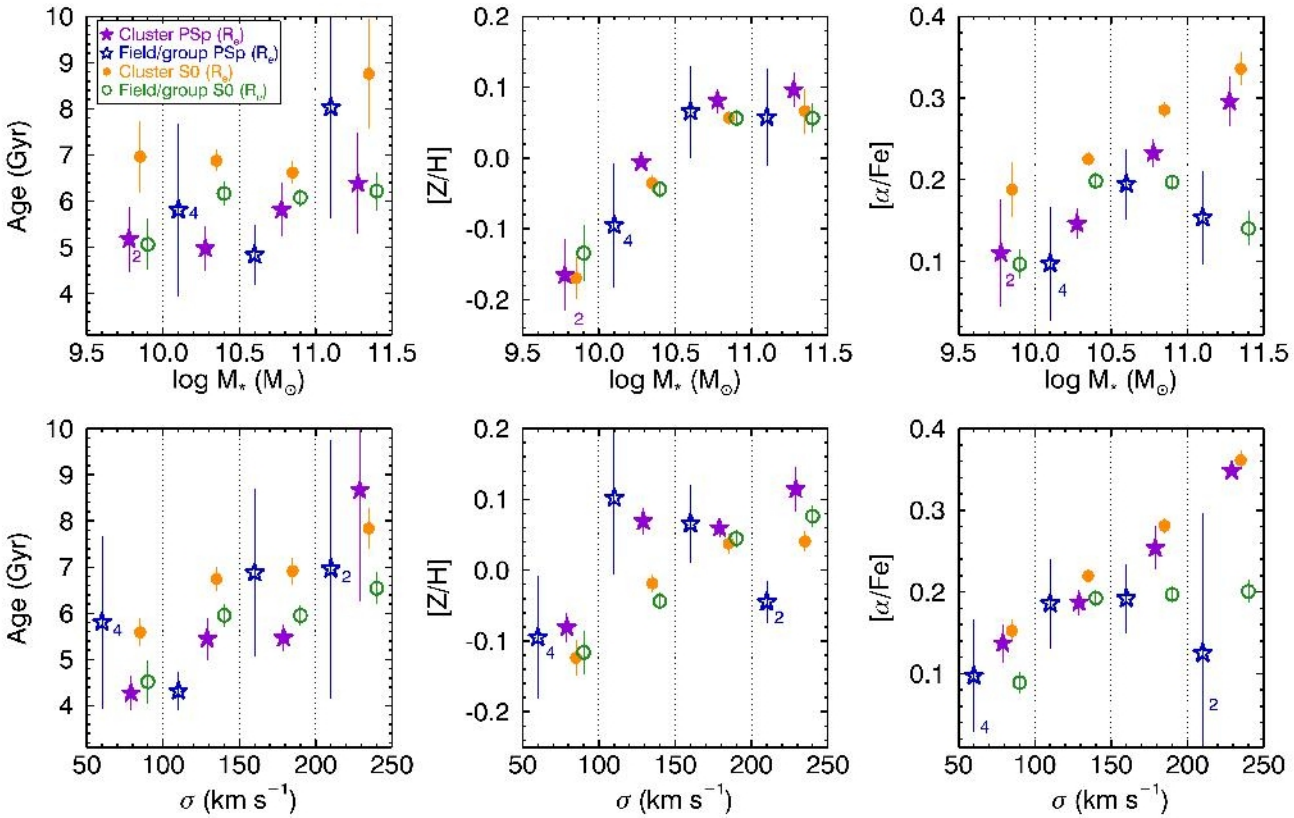

FIG. 9.— Mean age, [Z/H], and [α/Fe] in each mass (top panels) and $\sigma_\star$ (bottom panels) bin for all subdivisions as shown in the Figures

Зависимость от положения в фазовом пространстве скопления

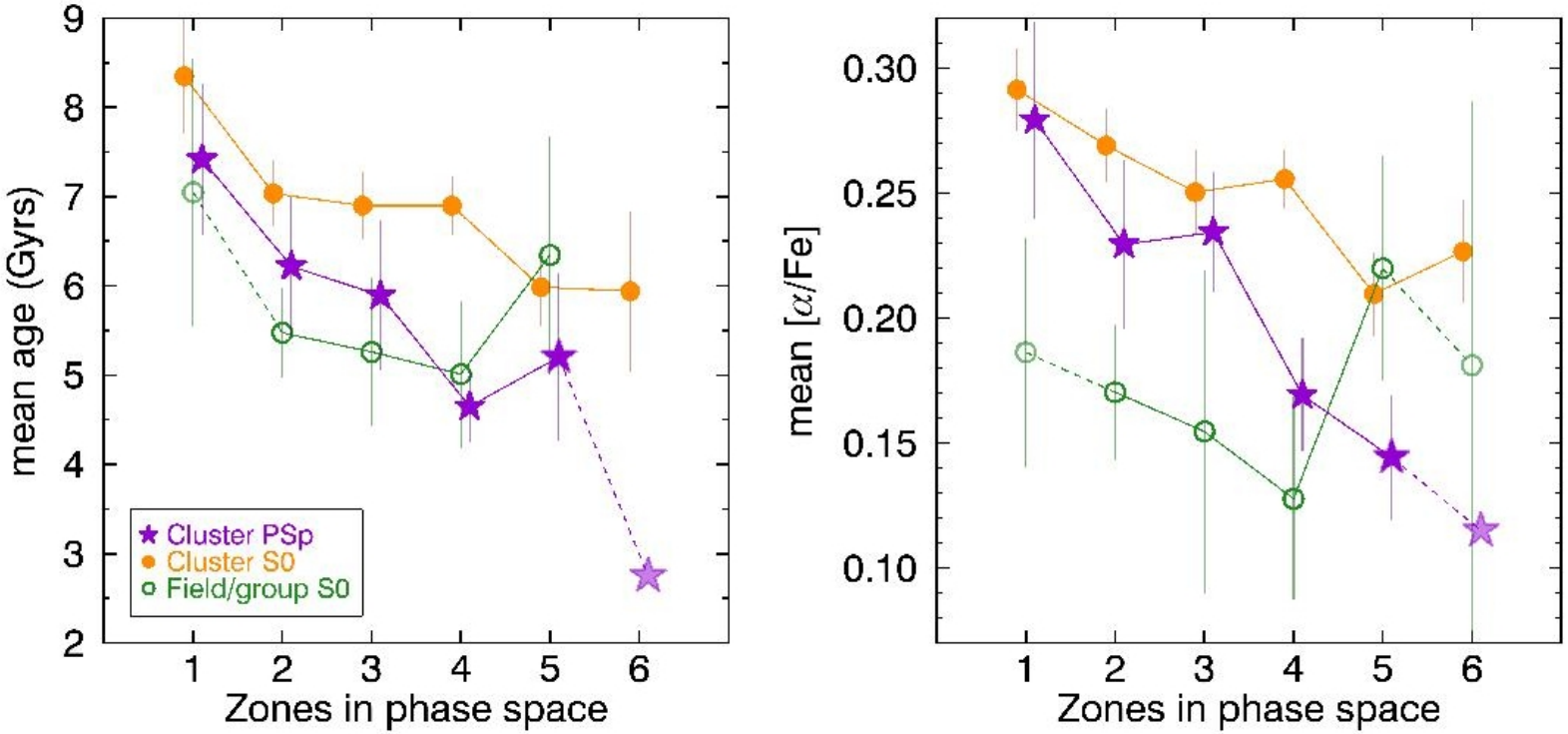

FIG. 12.— Mean age and [α/Fe] as a function of zone in projected phase-space presented by Figures 10 and 11. Stars are cluster passive spirals. Field/group passive spirals are not presented due to the small sample size (four galaxies). Orange filled and green open circles are cluster and field/group S0s, respectively. The error bar is the standard error of the mean. We connect to the symbols with dashed lines when the galaxies of each zone is less than 5.

ArXiv: 2011.04873

The SAMI Galaxy Survey: bulge and disk stellar population properties in cluster galaxies

S. Barsanti,[1,2] M. S. Owers,[1,2] R. M. McDermid,[1,2] K. Bekki,[3] J. Bland-Hawthorn,[4] S. Brough,[5,6] J. J. Bryant,[4,6,7] L. Cortese,[3,6] S. M. Croom,[4,6] C. Foster,[4,6] J. S. Lawrence,[8] Á. R. López-Sánchez,[1,6,8] S. Oh,[6,9] A. S. G. Robotham,[3,6] N. Scott,[4,6] S. M. Sweet,[6,10] and J. van de Sande[4,6]

[1] *Department of Physics and Astronomy, Macquarie University, NSW 2109, Australia*
[2] *Astronomy, Astrophysics and Astrophotonics Research Centre, Macquarie University, Sydney, NSW 2109, Australia*
[3] *ICRAR, The University of Western Australia, 35 Stirling Highway, Crawley, WA 6009, Australia*
[4] *Sydney Institute for Astronomy (SIfA), School of Physics, University of Sydney, NSW 2006, Australia*
[5] *School of Physics, University of New South Wales, NSW 2052, Australia*
[6] *ARC Centre of Excellence for All Sky Astrophysics in 3 Dimensions (ASTRO 3D), Australia*
[7] *Australian Astronomical Optics, AAO-USydney, School of Physics, University of Sydney, NSW 2006, Australia*
[8] *Australian Astronomical Optics - Macquarie, Macquarie University, NSW 2109, Australia*
[9] *Research School of Astronomy and Astrophysics, Australian National University, Canberra, ACT 2611, Australia*
[10] *School of Mathematics and Physics, University of Queensland, Brisbane, QLD 4072, Australia*

Submitted to ApJ. Accepted on November 9, 2020

ABSTRACT

We explore stellar population properties separately in the bulge and the disk of double-component cluster galaxies to shed light on the formation of lenticular galaxies in dense environments. We study eight low-redshift clusters from the Sydney-AAO Multi-object Integral field (SAMI) Galaxy Survey, using 2D photometric bulge-disk decomposition in the g, r and i-bands to characterize galaxies. For 192 double-component galaxies with $M_* > 10^{10}$ $M_\odot$ we estimate the color, age and metallicity of the bulge and the disk. The analysis of the $g-i$ colors reveals that bulges are redder than their surrounding disks with a median offset of 0.12 ± 0.02 mag, consistent with previous results. To measure mass-weighted age and metallicity we investigate three methods: (i) one based on galaxy stellar mass weights for the

Выборка

- Тоже спектры из обзора SAMI – поля обзора GAMA.
- 8 скоплений, 906 галактик $<R_{200}$, красные смещения 0:029 < z < 0:058.
- Фотометрия APMCC0917, EDCC0442, A3880 and A4038 – из 2dFGRS catalogue (De Propris et al. 2002); A85, A168, A119 and A2399 из SDSS.
- Разделение на балдж и диск – 469 галактик; из них 192 наблюдались SAMI (170 passive, 160 быстрые ротаторы, 146 классифицированы как S0…)

Характеристики

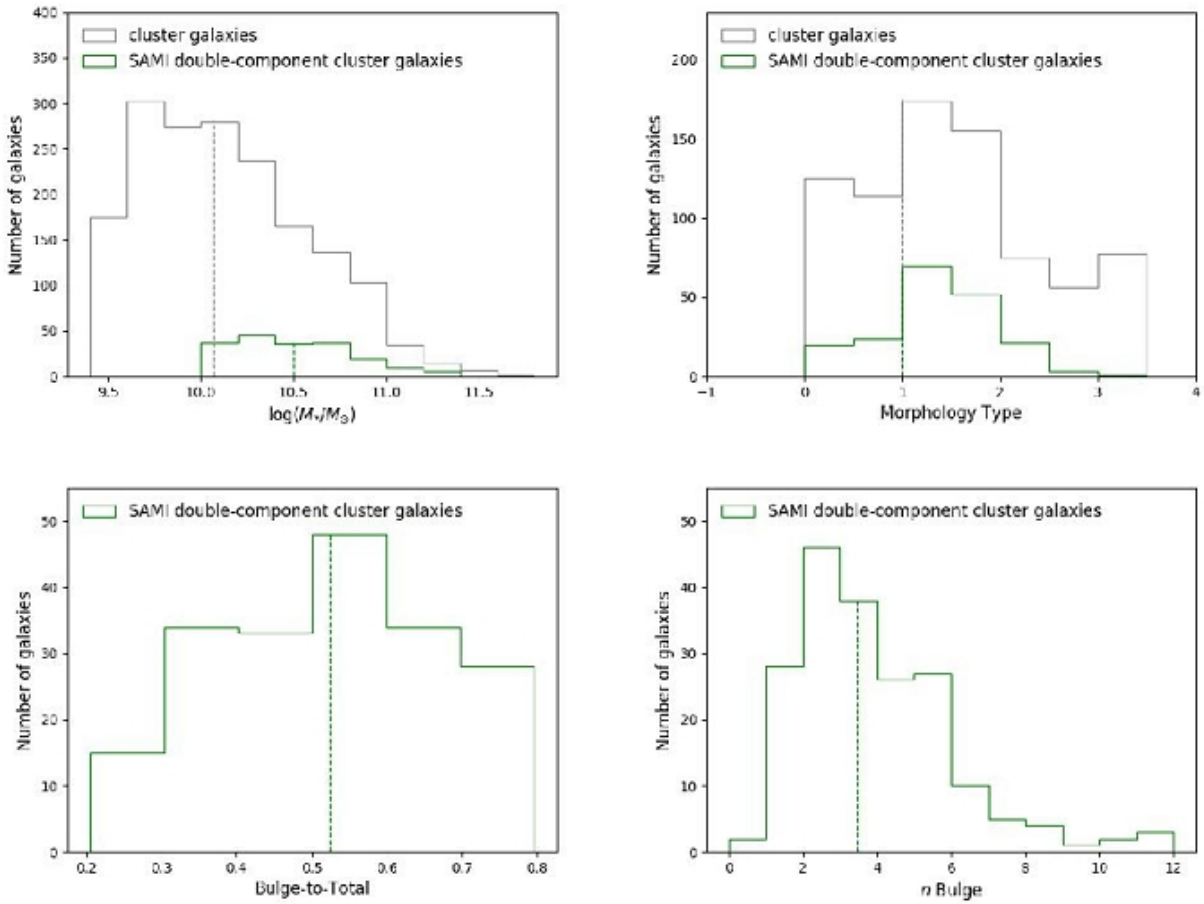

Figure 1. Distributions in M_*, morphology, bulge-to-total flux ratio and bulge Sérsic index for the 192 SAMI double-component galaxies. Stellar mass and morphology histograms are also plotted for the cluster galaxy sample of Barsanti et al. in preparation. The dashed lines represent the median values. The medians at morphology=1=S0, B/T=0.52 and n_{bulge} = 3.48 show the reliability of the model selection.

Как получить возраста и металличности для балджей и дисков

- Три метода: линейная комбинация с весами «вклад по массе», метод Эвелины Джонстон (в статье приписан Мендес-Абрё) и просто взять самые центральный бин и самый внешний бин.
- Бины (до 50 штук) – кольцевые, S/N>20.
- pPXF/SSP, green+red, аддитивный полином 12й степени,0.06<T<17.8 Gyr,

-2.32<[M/H]<+0.22…

- 109 уперлись в предел…

Пример: распределение параметров по бинам

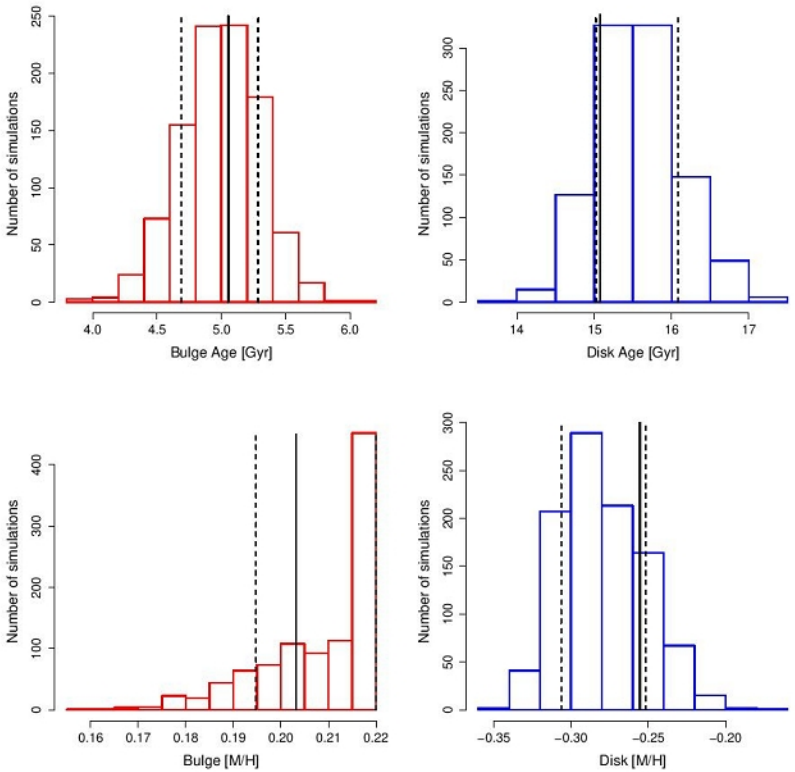

Figure 5. Age (*top panels*) and metallicity (*bottom panels*) distributions of bulge (red) and disk (blue) of the 9091700038 galaxy. The filled black line represents $Age_{bulge/disk}$ and $[M/H]_{bulge/disk}$, the dashed black lines are the associated uncertainties

А это пример приложения 2го метода…

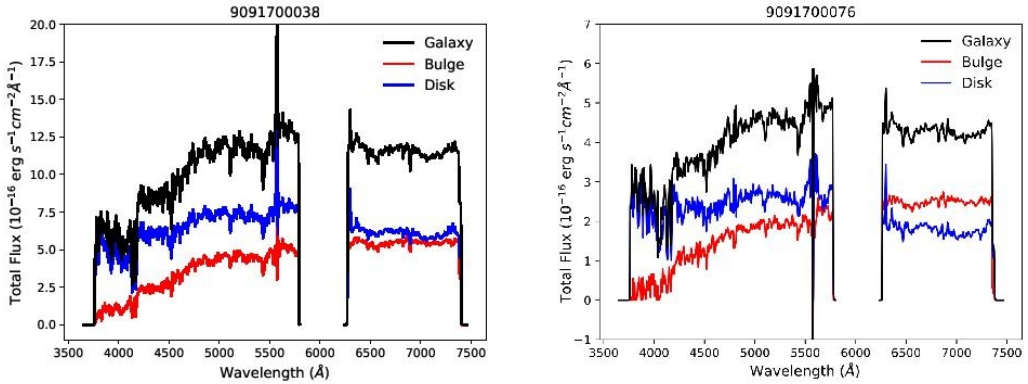

Figure 7. 1D spectra of the whole galaxy (black), the bulge (red) and the disk (blue) for the 9091700038 galaxy (*left panel*) and the 9091700076 galaxy (*right panel*), respectively.

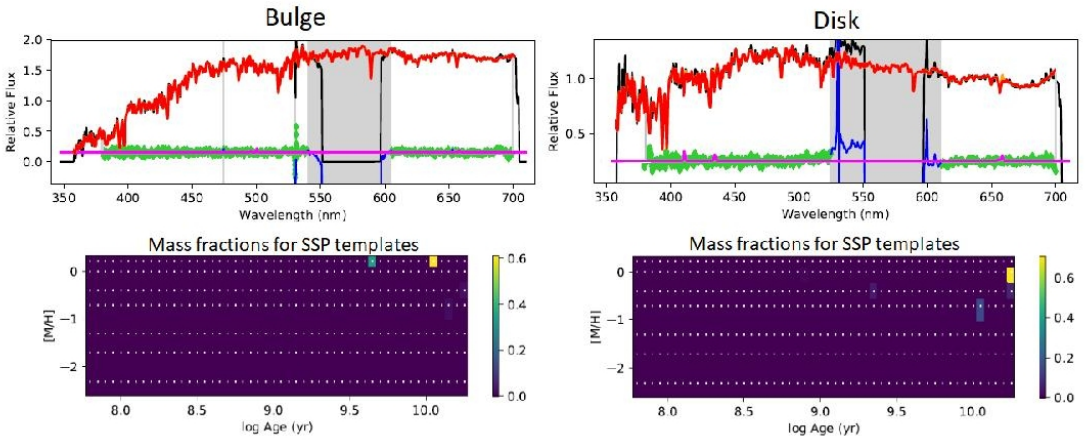

Figure 8. 1D bulge/disk spectra for the 9091700038 galaxy built with the method based on flux weights and fitted with pPXF.

Методы сравнивать – только расстраиваться…

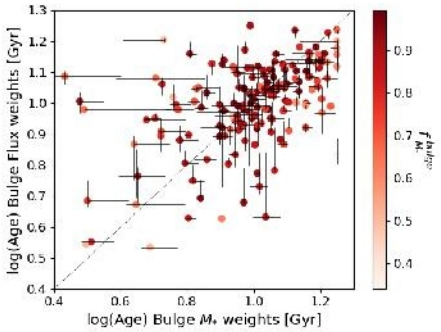

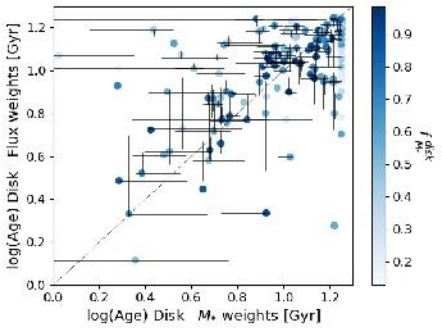

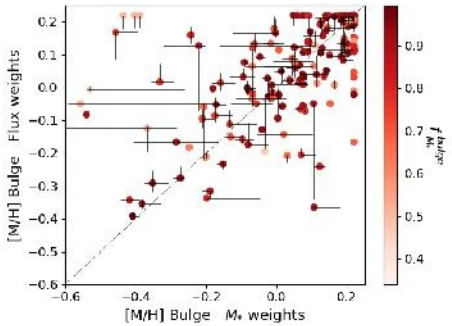

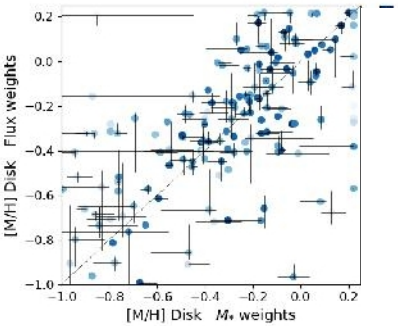

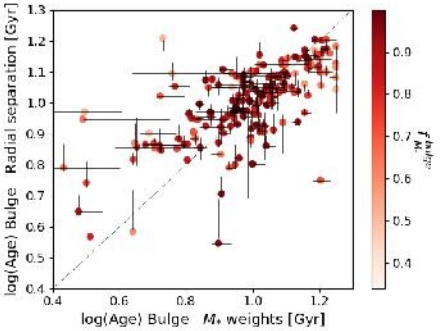

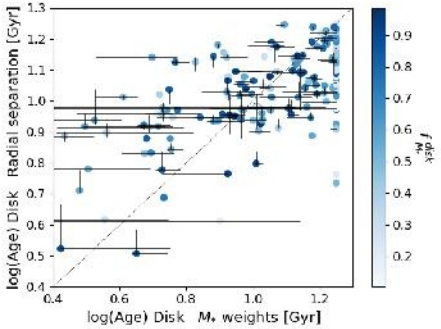

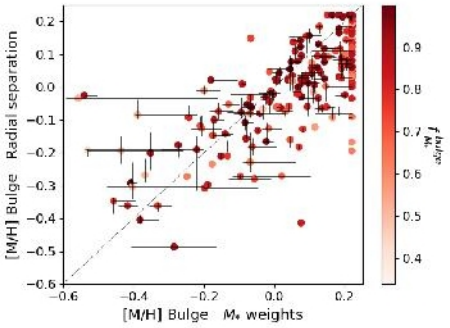

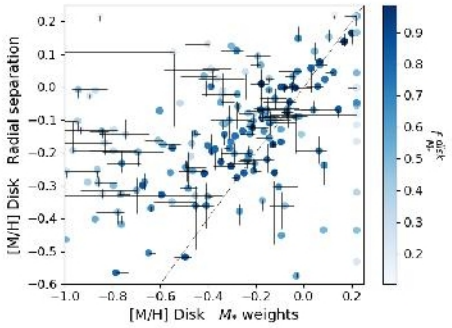

Результаты: балджи краснее дисков

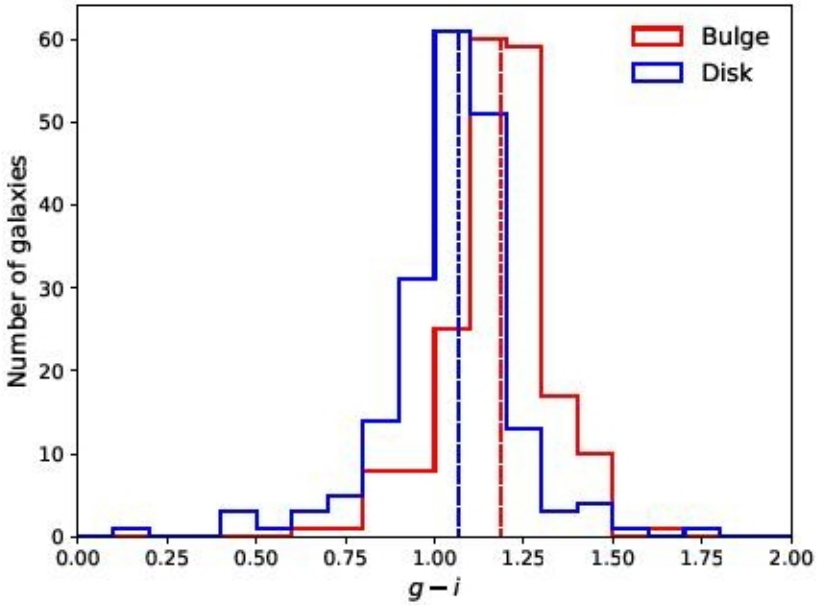

Figure 10. Histogram in $g - i$ color for the bulges (red) and the disks (blue) of the 192 SAMI cluster galaxies. The dashed lines represent the median values. Bulges have redder colors than disks.

Результаты: но балджи при этом часто моложе дисков…

Table 1. Differences in mass-weighted ages, metallicities and $(g-i)$ colors between bulges and disks from the three methods. Column 1 lists the method, column 2 the number of analyzed galaxies, columns 3/4/5/6/7/8 the percentages of galaxies with bulges older/younger/more metal-rich/more metal-poor/redder/bluer than the disks. The last line lists the average values for the three methods.

Method	N_g	%(Age) B>D	%(Age) B<D	%[M/H] B>D	%[M/H] B<D	%$(g-i)$ B>D	%$(g-i)$ B<D
M_* weights	192	45±4	55±4	80±3	20±3	73±3	27±3
Flux weights	181	45±4	55±4	86±3	14±3	73±3	27±3
Radial separation	54	43±7	57±7	81±5	19±5	67±6	33±6
Average		44±5	56±5	82±4	18±4	71±4	29±4

Table 2. Significant differences in bulge/disk mass-weighted ages and metallicities for the three methods. Column 1 lists lists the method, column 2 the number of analyzed galaxies, columns 3/4/5 the percentages of galaxies with bulges significantly older/younger/equal than the disks, and columns 6/7/8 the percentages of galaxies with bulges significantly more metal-rich/metal-poor/equal than the disks. The last line lists the average values for the three methods.

Method	N_g	%(Age) B$\gg$D	%(Age) B$\ll$D	%(Age) B$\sim$D	%[M/H] B$\gg$D	%[M/H] B$\ll$D	%[M/H] B$\sim$D
M_* weights	192	26±3	36±3	38±3	66±3	12±2	22±3
Flux weights	181	18±3	37±4	45±4	70±3	6±2	24±3
Radial separation	54	26±6	30±6	44±7	50±7	2±2	48±7
Average		23±4	34±4	43±5	62±4	7±2	31±4

Над этой картинкой надо долго размышлять…

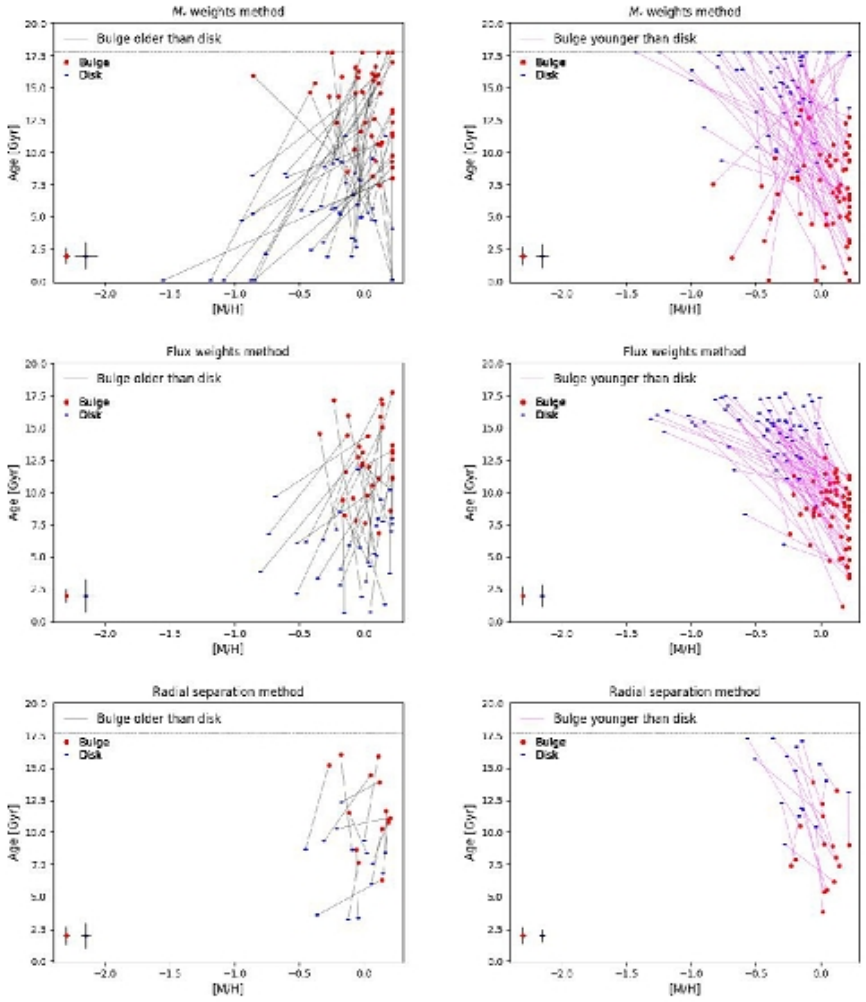

Figure 17. Age-metallicity plots for the three methods (*top to bottom panels*) where galaxies have the bulge significantly older (*left panels*) and younger (*right panels*) than the disk. The mean errors on the bulge and disk properties are plotted on the bottom left. In both galaxy populations, bulges are mainly more metal-rich compared to the disks, in agreement for the three methods.

Но никаких различий между галактиками с молодыми и старыми балджами нет!

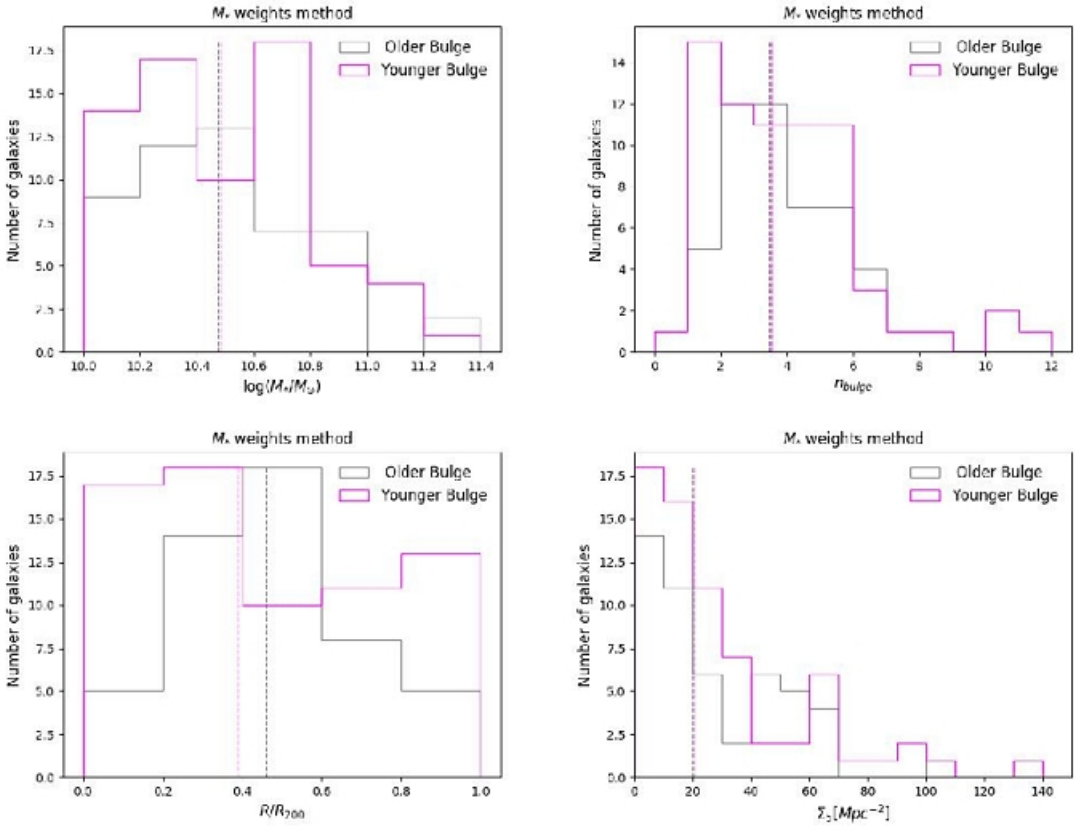

Figure 18. Histograms for the galaxies with a bulge significantly older (grey color) or younger (magenta color) than the disk as a function of the galaxy stellar mass (*top left panel*), bulge Sérsic index (*top right panel*), projected cluster-centric distance (*bottom left panel*) and galaxy density (*bottom right panel*). The dashed lines represent the median values. According to the Anderson−Darling test, we measure no significant differences.